

## ***In Vitro* Evaluation of Triazenes: DNA Cleavage, Antibacterial Activity and Cytotoxicity against Acute Myeloid Leukemia Cells**

**Vanessa O. Domingues,<sup>a</sup> Rosmari Hörner,<sup>\*,a</sup> Luiz G. B. Reetz,<sup>a</sup> Fábio Kuhn,<sup>a</sup>  
Virgínia M. Coser,<sup>b</sup> Jacqueline N. Rodrigues,<sup>b</sup> Rita Bauchspiess,<sup>b</sup>  
Waldir V. Pereira,<sup>b</sup> Gustavo L. Paraginski,<sup>c</sup> Aline Locatelli,<sup>c</sup>  
Juliana de O. Fank,<sup>c</sup> Vinícius F. Giglio<sup>c</sup> and Manfredo Hörner<sup>\*,c</sup>**

<sup>a</sup>Universidade Federal de Santa Maria, Departamento de Análises Clínicas e Toxicológicas,  
97105-970 Santa Maria-RS, Brazil

<sup>b</sup>Hospital Universitário de Santa Maria, Departamento de Hematologia-Oncologia,  
97105-970 Santa Maria-RS, Brazil

<sup>c</sup>Universidade Federal de Santa Maria, Departamento de Química, CP 5031,  
97105-970 Santa Maria-RS, Brazil

As diazoaminas assimétricas 1-(2-clorofenil)-3-(4-carboxifenil)triazeno (**1**), 1-(2-fluorofenil)-3-(4-carboxifenil)triazeno (**2**) e 1-(2-fluorofenil)-3-(4-amidofenil)triazeno (**3**) foram avaliadas quanto à capacidade de clivagem do DNA plasmidial pUC18 e pBSKII, atividade antibacteriana e citotoxicidade *in vitro* frente a células de leucemia mielóide aguda e leucócitos normais utilizando o bioensaio da redução do sal brometo de 3-(4,5-dimetiltiazol-2-il)-2,5-difeniltetrazólio (MTT). Os triazenos analisados demonstraram capacidade de clivagem dos dois tipos de DNA plasmidial: triazeno **1** em pH 8,0 e 50 °C; triazeno **2** em pH 6,5 a 37 e 50 °C; triazeno **3** em pH 6,5 e 37 °C. Os compostos apresentaram atividade citotóxica frente a células leucêmicas. O composto **1** mostrou alta atividade frente a *B. cereus* (CIM = 32 µg mL<sup>-1</sup>). A associação molecular através de ligações de hidrogênio no estado sólido do composto **3** com base na análise estrutural por difratometria de raios X em monocristal, bem como os resultados das análises espectroscópicas nas regiões do IV e UV-Vis dos compostos **1**, **2** e **3** são discutidos no presente trabalho.

The asymmetric diazoamines 1-(2-chlorophenyl)-3-(4-carboxyphenyl)triazene (**1**), 1-(2-fluorophenyl)-3-(4-carboxyphenyl)triazene (**2**) and 1-(2-fluorophenyl)-3-(4-amidophenyl)triazene (**3**) were evaluated for their ability to cleave pUC18 and pBSKII plasmid DNA, antibacterial activity and *in vitro* cytotoxicity against acute myeloid leukemia cells and normal leukocytes using the bioassay of reduction of 3-(4,5-dimethylthiazol-2-yl)-2,5-diphenyltetrazolium bromide (MTT). The triazenes showed ability to cleave the two types of plasmid DNA: triazene **1** at pH 8.0 and 50 °C; triazene **2** at pH 6.5 and 37 and 50 °C; triazene **3** at pH 6.5 and 37 °C. The compounds presented cytotoxic activity against myeloid leukemia cells. Compound **1** showed high activity against *B. cereus* (MIC = 32 µg mL<sup>-1</sup>). The observation of intermolecular hydrogen bonding in the solid state of compound **3**, based on the structural analysis by X-ray crystallography, as well as the results of IR and UV-Vis spectroscopic analyses of compounds **1**, **2** and **3** are discussed in the present work.

**Keywords:** triazenes, DNA cleavage, antibacterial activity, cytotoxicity

### **Introduction**

Triazenes or diazoamines constitute a class of compounds containing three consecutive nitrogen atoms

in an acyclic arrangement.<sup>1</sup> Diazoamino compounds can be obtained by diverse synthetic ways, the classical method including the coupling reaction of a diazonium salt, [R-N≡N]<sup>+</sup>X<sup>-</sup>, with an amine (R'-NH<sub>2</sub>) in acidic medium. This is followed by formation of the respective diazoamino compound R-N=N-N(H)-R' (R = R' for

\*e-mail: rosmari.ufsm@gmail.com, hoerner.manfredo@gmail.com

symmetric triazenes;  $R \neq R'$  for asymmetric compounds) by stepwise neutralization of the reaction system. They have diverse applications as DNA alkylating agents in tumor therapy, protecting groups in natural product synthesis and combinatorial chemistry, as well as precursors incorporated into polymer and oligomer synthesis.<sup>2-8</sup>

Hydrolysis of DNA or RNA catalyzed by relevant enzymes is an important subject in biotechnology, medicine and drug development.<sup>9,10</sup> Synthetic nucleases which rapidly cleave nucleic acids under mild conditions have many important potential applications ranging from the synthesis of custom-designed artificial restriction enzymes to the development of new antitumor agents.<sup>11</sup> To mimic the biological function of enzymes, triazene compounds that cleave DNA are interesting for the development of artificial nucleases. In this context, *N*-(3-hydroxypropyl)berenil represents one example of a triazene capable to promote DNA cleavage.<sup>12</sup>

Triazenes also act as chemotherapeutic agents for many tumors, such as brain, leukemia, melanoma, lymphoma and sarcoma.<sup>13-17</sup> Among all chemotherapeutic agents tested against metastatic melanoma, DTIC (5-(3,3-dimethyltriazene)imidazol-4-carboxamide) – an FDA-approved pro-drug activated by *N*-demethylation in liver microsomes (microsomal enzyme CYP450) – is the most active single agent and thus considered a reference drug.<sup>18,19</sup>

Temozolomide (TMZ), *i.e.*, 8-carbamoyl-3-methylimidazol[5,1-*d*]-1,2,3,5-tetrazin-4(3*H*)-one, is another example of a methylating triazene like DTIC, which acts under physiological conditions against primary and metastatic tumors in the brain.<sup>20</sup> Despite the need for more clinical experiments for the use of triazene compounds in acute leukemia and myelodysplasia treatments, some studies have shown that both DTIC and TMZ have antineoplastic activity in patients with leukemia.<sup>21-23</sup>

Recently the antimicrobial susceptibility profile of fifteen triazenes was evaluated by our group based on the reference broth microdilution method according to CLS guidelines.<sup>24</sup>

The mechanism of cytotoxicity of triazenes involves mainly methylation of the  $O^6$  position of guanine in DNA.<sup>25</sup> On the other hand, it is well known that molecular association plays an important role in biological systems. Strategic modifications of electronic and geometric characteristics applied in molecular design determine the dimensionality of molecular association by diverse types of intermolecular secondary non-bonding interactions such as the large palette of hydrogen bonding. Hydrogen bonding is an important non-covalent interaction in structural investigations relative to molecular recognition and reactivity of molecules with

biological importance. From this point of view, diverse biological reaction mechanisms can be related to hydrogen bonding due to its energy range situated between van der Waals interactions and covalent bonds.<sup>26,27</sup>

The present study deals with the synthesis and characterization of 1-(2-chlorophenyl)-3-(4-carboxyphenyl) triazene (**1**), 1-(2-fluorophenyl)-3-(4-carboxyphenyl) triazene (**2**) and 1-(2-fluorophenyl)-3-(4-amidophenyl) triazene (**3**) (Figure 1). The study also demonstrates that the compounds are able to cleave pUC18 and pBSKII plasmid DNA through a possible hydrolytic mechanism. The antibacterial activity and *in vitro* cytotoxicity of the three triazenes against acute myeloid leukemia (AML) cell lines and control cell (without AML) using the bioassay of reduction of 3-(4,5-dimethylthiazol-2-yl)-2,5-diphenyltetrazolium bromide (MTT) are also analyzed. The single crystal structural analysis of 1-(2-fluorophenyl)-3-(4-amidophenyl) triazene (**3**), including its self-assembly in the solid state through hydrogen bonding, and the vibrational and electronic spectra of compounds **1**, **2** and **3** are also presented.

## Experimental

### Materials

All reagents and solvents used in the study were reagent grade and were used without further purification. For biological assays, water was purified by passage through a Millipore water purification system with a resistance of 18 M $\Omega$  and sterilized by autoclave. Reaction solutions for DNA cleavage studies, determination of minimum inhibitory concentrations and cytotoxicity essays were prepared according to standard sterile techniques. The DNA bands were stained, visualized on a UV transilluminator at 254 nm, photographed using a digital photographic camera and quantified using Scion Image Beta 4.03 software (Scion Corp.).

<sup>1</sup>H and <sup>13</sup>C NMR spectra were recorded on a Bruker DPX 200 instrument. IR spectra were recorded on a Bruker FT-IR Spectrometer TENSOR 27 instrument with samples embedded in KBr pellets. UV-Vis spectra were measured on a Shimadzu UV-1650-PC spectrophotometer.

### Synthesis of 1-(2-chlorophenyl)-3-(4-carboxyphenyl) triazene (**1**)

The synthesis of triazene **1** was formerly reported in 1956.<sup>28</sup> The preparation was made with a solution of 4-aminobenzoic acid (1.00 g, 7.30 mmol) in 10 mL HCl 6 mol L<sup>-1</sup> previously cooled to -2 °C and added throughout 10 min, under continuous stirring, to a solution of sodium

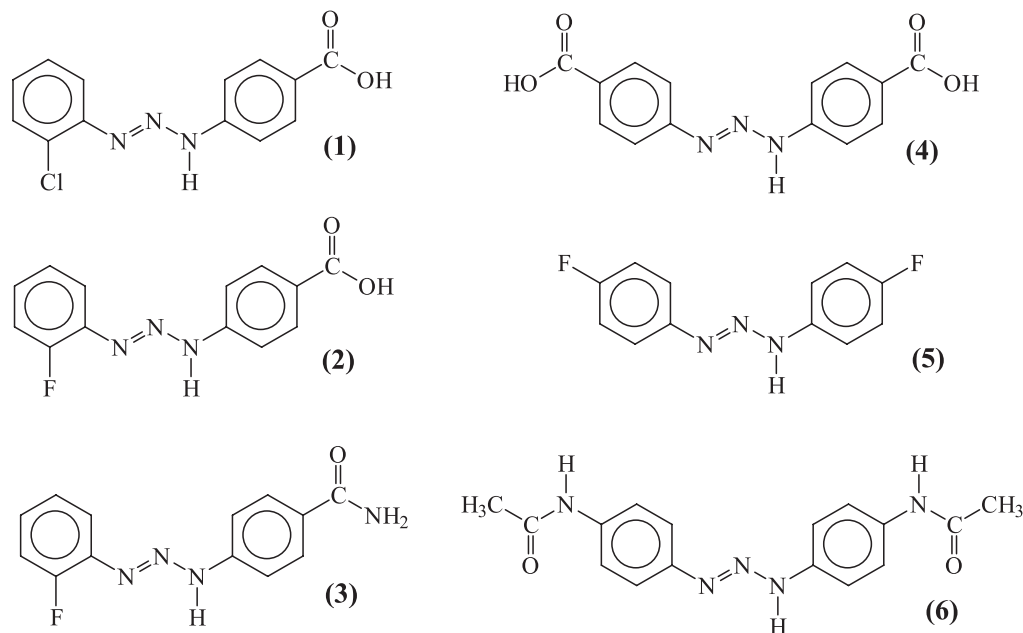


**Figure 1.** Molecular structure of 1-(2-chlorophenyl)-3-(4-carboxyphenyl)triazene (**1**), 1-(2-fluorophenyl)-3-(4-carboxyphenyl)triazene (**2**), 1-(2-fluorophenyl)-3-(4-amidophenyl)triazene (**3**), 1,3-bis(4-carboxyphenyl)triazene (**4**), 1,3-bis(4-fluorophenyl)triazene (**5**) and 1,3-bis(4-acetamidophenyl)triazene(**6**).

nitrite (0.60 g, 8.70 mmol) in water (10 mL). The reaction mixture was kept at  $-2\text{ }^{\circ}\text{C}$  and a solution of 2-chloroaniline (0.93 g, 7.30 mmol) in  $6\text{ mol L}^{-1}$  HCl (5 mL) was slowly added under continuous stirring. Stirring was continued for 20 min at a temperature between  $-2$  and  $-5\text{ }^{\circ}\text{C}$ . A cold sodium acetate solution (10%) was then added in small amounts until pH 7.0 was reached while a yellow solid precipitated. The crude product, separated by filtration, was washed with small amounts of cold water and purified by column chromatography after its adsorption onto silica gel (70/230 mesh) using 5% acetone in hexane as eluent. The yellow product, in form of fine microcrystalline needles, was dried under vacuum. Yield 53% (0.95 g, 3.84 mmol) based on 4-aminobenzoic acid, mp  $172\text{ }^{\circ}\text{C}$ ; IR  $\nu_{\text{max}}/\text{cm}^{-1}$ , KBr pellets: 3174 (N–H), 2986 (O–H), 1682 (C=O), 1597 (C=C), 1510 ( $\delta$ (N–H), deformation), 1430 ( $\delta$ (O–H), deformation in plane), 1414 (N=N), 1312 (C–O), 1209 (N–N), 756 ( $\delta$ (C–H), deformation).  $^1\text{H NMR}$  (200 MHz,  $\text{dms-}d_6/\text{tms}$ )  $\delta$  12.33 (br, s, 1H, OH), 7.16–7.70 (m, 8H, Ph);  $^{13}\text{C NMR}$  (200 MHz,  $\text{dms-}d_6$ )  $\delta$  146.6 (C=O), 130.6, 129.4, 129.2, 129.0, 128.9, 128.5, 125.4, 121.4, 121.3, 120.1, 119.4, 119.2 (Ph);  $\lambda_{\text{max}}/\text{nm}$  (MeOH) 203, 242, 361 ( $\epsilon/\text{dm}^3\text{ mol}^{-1}\text{ cm}^{-1}$   $18.6 \times 10^3$ ).

#### Synthesis of 1-(2-fluorophenyl)-3-(4-carboxyphenyl) triazene (**2**)

To a solution of 4-aminobenzoic acid (1.00 g, 7.30 mmol) in 10 mL  $6\text{ mol L}^{-1}$  HCl previously cooled to  $-2\text{ }^{\circ}\text{C}$ , a

sodium nitrite solution (0.60 g, 8.70 mmol) in water (10 mL) was added under continuous stirring throughout 10 min. The reaction mixture was kept at  $-2\text{ }^{\circ}\text{C}$  and a solution of 2-fluoroaniline (0.81 g, 7.30 mmol) in  $6\text{ mol L}^{-1}$  HCl (5 mL) was slowly added under continuous stirring. Stirring was continued for 20 min at a temperature between  $-2$  and  $-5\text{ }^{\circ}\text{C}$ . A cold sodium acetate solution (10%) was then added in small amounts until pH 7.0 was reached while a yellow solid precipitated. The crude product, separated by filtration, was washed with small amounts of cold water and purified by column chromatography after its adsorption onto silica gel (70/230 mesh) using diethyl ether as eluent. The yellow product in form of fine microcrystalline needles was dried under vacuum. Yield 64% (1.21 g, 4.70 mmol) based on 4-aminobenzoic acid, mp  $175\text{ }^{\circ}\text{C}$ . IR  $\nu_{\text{max}}/\text{cm}^{-1}$ , KBr pellets: 3175 (N–H), 2985 (O–H), 1680 (C=O), 1607 (C=C), 1491 ( $\delta$ (N–H), deformation), 1431 ( $\delta$ (O–H), deformation in plane), 1404 (N=N), 1312 (C–O), 1201 (N–N), 756 ( $\delta$ (C–H), deformation).  $^1\text{H NMR}$  (200 MHz,  $\text{dms-}d_6/\text{tms}$ )  $\delta$  13.06 (br, s, 1H, OH), 7.21–7.96 (m, 8H, Ph);  $^{13}\text{C NMR}$  (200 MHz,  $\text{dms-}d_6$ )  $\delta$  166.9 (C=O), 131.1, 128.5, 128.4, 124.9, 124.8, 119.1, 116.8, 116.4, 114.0 (Ph);  $\lambda_{\text{max}}/\text{nm}$  (MeOH) 202, 237, 361 ( $\epsilon/\text{dm}^3\text{ mol}^{-1}\text{ cm}^{-1}$   $21.9 \times 10^3$ ).

#### Synthesis of 1-(2-fluorophenyl)-3-(4-amidophenyl) triazene (**3**)

To a solution of 2-fluoroaniline (0.89 g, 8.01 mmol) in 10 mL of  $6\text{ mol L}^{-1}$  HCl previously cooled to  $-2\text{ }^{\circ}\text{C}$ , a

sodium nitrite solution (0.58 g, 8.41 mmol) in water (5 mL) was added under continuous stirring throughout 10 min. The reaction mixture was kept at  $-2\text{ }^{\circ}\text{C}$  and a solution of 4-aminobenzamide (1.09 g, 8.00 mmol) in acetone (10 mL) was slowly added under continuous stirring. Stirring was continued for 20 min at a temperature between  $-2$  and  $-5\text{ }^{\circ}\text{C}$ . A cold concentrated sodium carbonate solution was then added in small amounts until pH 7.0 was reached while a yellow solid precipitated. The crude product, separated by filtration, was washed with small amounts of cold water, followed by small amounts of cold ethanol and purified by column chromatography after its adsorption onto silica gel (70/230 mesh) using hexane:ethyl acetate (3:7) as eluent. The microcrystalline product was recrystallized from a hexane:ethyl acetate mixture (1:3). Yellow vitreous bar-shaped crystals of **3** suitable for X-ray diffraction analysis were obtained by slow evaporation of the solvent mixture within five days. Yield 86% (1.48 g, 5.7 mmol) based on 2-fluoroaniline, mp  $200\text{ }^{\circ}\text{C}$ . IR  $\nu_{\text{max}}/\text{cm}^{-1}$ , KBr pellets: 3493 (N–H, amide), 3404 (N–H, amide), 3167 (N–H, amine), 1665 (C=O), 1611 (C=C), 1489 ( $\delta$ (N–H), deformation), 1427 ( $\delta$ (O–H), deformation in plane), 1391 (N=N), 1312 (C–O), 1202 (N–N), 752 ( $\delta$ (C–H), deformation).  $^1\text{H}$  NMR (200 MHz,  $\text{dms}\text{-}d_6/\text{tms}$ )  $\delta$  13.05 (br, s, 1H, OH), 7.22–7.97 (m, 8H, Ph);  $^{13}\text{C}$  NMR (200 MHz,  $\text{dms}\text{-}d_6$ )  $\delta$  167.9 (C=O), 144.4, 129.6, 129.1, 128.8, 125.4, 125.3, 119.6, 117.2, 116.9, 114.0 (Ph);  $\lambda_{\text{max}}/\text{nm}$  (MeOH) 202, 233, 361 ( $\epsilon/\text{dm}^3\text{ mol}^{-1}\text{ cm}^{-1}$   $26.7 \times 10^3$ ).

#### DNA cleavage studies

DNA cleavage was measured by the conversion of supercoiled pUC18 and pBSKII plasmid DNA (Stratagene) to nicked circular and linear DNA forms. The screening assay to achieve nucleic acids cleavage was performed in a final volume of 20  $\mu\text{L}$  where the following reagents were present: 1  $\mu\text{g}$  of plasmid DNA and different concentrations of tested compounds (3.75, 1.875, 1.25, 0.75 and 0.375  $\text{mmol L}^{-1}$ ) at pH 6.5 (200  $\text{mmol L}^{-1}$  PIPES buffer) and 8.0 (200  $\text{mmol L}^{-1}$  Tris-HCl buffer) at 37 and 50  $^{\circ}\text{C}$  for 24 h; all assays were made twice. Samples were submitted to agarose gel (0.8%) electrophoresis stained with ethidium bromide. The resulting gels were digitalized with a photodocumentation system.

In order to verify the probable mechanism of DNA strand scission, the assays were repeated in the presence of free radical scavengers (thiourea 40  $\text{mmol L}^{-1}$ , glycerol 0.1% and 1.0% and dimethyl sulfoxide 0.04  $\text{mol L}^{-1}$ ) in the same cleavage conditions (pUC18 and pBSKII plasmids at pH 6.5 and 8.0, 37 and 50  $^{\circ}\text{C}$  for 24 h). Cleavage assays were also performed in argon atmosphere in order to verify

the cleavage ability in absence of atmospheric oxygen according to the methodology described.<sup>29</sup>

#### Bacterial strains

*In vitro* antimicrobial activities of the triazene compounds were evaluated against 30 test organisms, including 14 Gram-positive and 16 Gram-negative bacterial strains. The groups included nine bacteria of the American Type Culture Collection (ATCC): *Pseudomonas aeruginosa* ATCC 27853, *Escherichia coli* ATCC 25922, *Escherichia coli* ATCC 35218, *Salmonella choleraesuis* ATCC 10708, *Klebsiella pneumoniae* ATCC 700603, *Staphylococcus aureus* ATCC 25923, *Staphylococcus epidermidis* ATCC 12228, *Enterococcus faecalis* ATCC 29212 and *Bacillus cereus* ATCC 10987. Twenty one clinical bacteria from the Microbiology Laboratory of the Hospital Universitário de Santa Maria, Brazil, were identified by a Siemens MicroScan automated system: *Shigella sonnei*, *Enterobacter cloacae*, *Klebsiella oxytoca*, *Bacillus cereus*, *Micrococcus* sp., *Streptococcus pyogenes*, *Acinetobacter baumannii*, *Ralstonia pickettii*, *Serratia marcescens*, *Enterococcus* sp., *Listeria monocytogenes*, *Aeromonas hydrophyla*, *Enterobacter aerogenes*, *Streptococcus agalactiae*, *Salmonella tiphymurium*, *Corynebacterium* sp., *Salmonella* sp., *Staphylococcus epidermidis*, *Acinetobacter lwoffii*, *Klebsiella pneumoniae*, *Staphylococcus hominis* subsp. *hominis*.

#### Determination of minimum inhibitory concentrations (MICs)

Antimicrobial susceptibility testing was performed by the broth microdilution method using cation-supplemented Mueller Hinton broth (Difco, Detroit, MI), according to Clinical and Laboratory Standards Institute (CLSI) guidelines.<sup>30</sup> Inoculum suspensions were prepared by diluting the broth culture supernatant with sterile saline with density of 0.5 (McFarland standard) using a spectrophotometer (Bausch & Lomb Spectronic 20). All compounds were tested at concentrations ranging from 0.125 to 128  $\mu\text{g mL}^{-1}$  and dissolved in 20% of EtOH. The plates were incubated without agitation at  $35 \pm 2\text{ }^{\circ}\text{C}$  for 24 h. The technique is based on the growth of the test organisms (inoculums + compounds) relative to a positive control (bacteria without compound), with addition, after 24 h, of 10  $\mu\text{L}$  of 2% 2,3,5-triphenyltetrazolium chloride (TTC). TTC is colorless in the oxidized form and red when reduced. Live microorganisms reduce TTC by enzymatic action, originating formazan kept inside granules in the cells, which become red.<sup>31</sup> MIC values were defined as the lowest concentration

of the triazene compounds that inhibited visible growth of microorganisms. All tests were made three times.

### Cell lines

Leukemic cells were obtained from three acute myeloid leukemia patients without treatment diagnosed at the Hematology-Oncology Laboratory of the Hospital Universitário de Santa Maria, Brazil, by light microscopic examination of the bone marrow as well as flow cytometry to diagnose the presence of leukemia, to differentiate AML from other types of leukemia and to classify the subtype of disease. Cell lines of control patient (without AML) was obtained by collecting peripheral blood with EDTA. The mononuclear cells from bone marrow (1 mL) and peripheral blood (6 mL) were isolated by Ficoll-Paque PLUS (Sigma) density separation (centrifuged at 4000 rpm for 20 min). After isolation, the cells were washed three times in RPMI-1640 (Sigma) and the erythrocytes were lysed with hemolytic buffer. The cells were grown in RPMI with 20% fetal bovine serum (Sigma), penicillin 100 U mL<sup>-1</sup>, streptomycin 100 µg mL<sup>-1</sup>, HEPES buffer and sodium bicarbonate during 24 h at 37 °C, with 5% CO<sub>2</sub>.

### MTT assay

MTT was dissolved in phosphate buffered saline (PBS) at 5 mg mL<sup>-1</sup> and filtered to sterilize and remove a small amount of insoluble residue. Trypan blue (1% in distilled water) and cell suspensions were mixed in 1:6 quantities (50 µL of cells + 10 µL trypan blue). The quantity of cells was estimated by hemocytometry and (blue) stained cells were scored as dead. About 3 × 10<sup>6</sup> cells mL<sup>-1</sup> were grown with compounds for 24 h at 37 °C and 5% CO<sub>2</sub>. The triazene doses varied from 12.5, 50 and 100 µmol mL<sup>-1</sup>; the compounds were dissolved in dimethyl sulfoxide, which did not exceed 0.25% in the cell cultures. The DTIC solution was prepared in water. The microculture plates included 90 µL cell suspension and 10 µL of the compound solution. Control cultures received cells in absence of assayed compounds. After 20 h the MTT solution was added to all wells and plates were incubated at 37 °C for 4 h. At the end of the incubation period, the formazan product was dissolved in 100 µL of dimethyl sulfoxide. The optical density (OD) of each well was measured using a Fisher Bio-Tek BT2000 MicroKinetics reader (λ = 570 nm). Each assay was carried out three times. The cell survival fraction was calculated by the following equation:

$$\text{Cell survival} = (\text{OD of the treated well} / \text{mean OD of the control wells}) \times 100\%$$

The IC<sub>50</sub> value, defined as the drug concentration causing a 50% reduction in cellular viability, was calculated for each compound. The experimental data were transformed to sigmoid dose-response curves using nonlinear regression analysis (GraphPad Prism 5), which enabled the calculation of the corresponding IC<sub>50</sub>.

### Crystal structure determination

A single crystal on a glass fiber was used for the X-ray data collection. Data were collected at -123 °C with a Bruker APEX II CCD area-detector diffractometer and graphite monochromatized Mo-K<sub>α</sub> radiation using COSMO program.<sup>32</sup> No crystal decay was observed. Crystal system and space group were unequivocally determined from the data sets and reciprocal space images. Cell refinement, data reduction and absorption correction were performed using SAINT and SADABS programs, respectively.<sup>32</sup> The structure of **3** was solved by direct methods and refined on *F*<sup>2</sup> with anisotropic temperature parameters for all non-hydrogen atoms.<sup>33,34</sup> The H atoms in the structure of **3** were identified in Fourier difference maps and refined as individual atoms with isotropic displacement parameters. Table 1 shows the crystallographic data and details of data collection and refinement, and Table 2 the selected bond lengths and angles. Graphical representations were drawn with the DIAMOND software.<sup>35</sup>

## Results and Discussion

### Spectroscopic characterization

#### Infrared spectra

The infrared spectra of **1**, **2** and **3** were analyzed in the spectral region 4000-400 cm<sup>-1</sup>. The main absorptions and vibrational assignments were compared with literature data.<sup>36-38</sup> Amide derivatives are characterized by two absorptions in sequence with medium intensities and 120-200 cm<sup>-1</sup> spacing in the 3550-3150 cm<sup>-1</sup> region. In compound **3** these absorptions were assigned at 3493 and 3404 cm<sup>-1</sup>.<sup>36,37</sup> The shift to lower frequency can be attributed to electronic delocalization towards the terminal aryl substituents of the [-N=N-N(H)-] diazoamino group. The characteristic N-H stretching at 3181 cm<sup>-1</sup> for the [-N=N-N(H)-] triazene group was observed as weak to medium signals at 3167-3175 cm<sup>-1</sup> in **1**, **2** and **3**. Compared with 1,3-bis(phenyl) triazene the [-N=N-N(H)-] diazoamino group in **1**, **2** and **3** was undoubtedly characterized by strong absorptions at 1489-1510 cm<sup>-1</sup>, 1391-1414 cm<sup>-1</sup> and 1201-1208 cm<sup>-1</sup> corresponding to N-H in plane deformation, ν<sub>as</sub>(N=N) and ν<sub>s</sub>(N-N), respectively.<sup>38</sup>

Compounds **1** and **2** could be analyzed as R–C(=O)OH carboxylic derivatives, usually characterized in the solid state by a strong, very broad O–H stretching near 3000 cm<sup>-1</sup>.<sup>36</sup> In compounds **1** and **2** this broad band was observed at 2986 and 2985 cm<sup>-1</sup>, respectively. In compound **3** this absorption was absent. Carboxylic acids and derivatives usually exist as (R–C=O...H–O–C–R)<sub>2</sub> hydrogen-bonded dimers. If the dimer unit is considered, two carbonyl stretching frequencies, symmetric and asymmetric, are observed. The former is Raman active, and the asymmetric will be IR active only, assigned for most carboxyl dimers at 1720–1680 cm<sup>-1</sup>.<sup>36</sup> Such observation agrees with the absorptions observed at 1665–1682 cm<sup>-1</sup> assigned to  $\nu_{\text{as}}(\text{C}=\text{O})$  for **1**, **2** and **3**. Further, the carboxyl dimer presents a characteristic infrared band at 960–875 cm<sup>-1</sup> which corresponds to out-of-plane OH...O hydrogen deformation.<sup>36</sup> In the case of **1** and **2**, this characteristic absorption is observed near 850 cm<sup>-1</sup> probably due to electronic delocalization towards the terminal aryl substituents of the [–N=N–N(H)–] diazoamino group. In the case of **3** the crystal structure shows intermolecular associations promoted by C–O...H–N hydrogen bonding between the carbonyl group of the amido substituent and the [–N=N–N(H)–] diazoamino group (Figure 3), which can be associated to the out-of-plane OH...N hydrogen deformation in analogy with the out-of-plane OH...O hydrogen deformation of R–C(=O)OH derivatives. This explains the well-defined absorption observed at 843 cm<sup>-1</sup> in the spectra of **3**. Besides the characteristic out-of-plane OH...O hydrogen deformation, (R–C=O...H–O–C–R)<sub>2</sub> carboxyl dimers are characterized by O–H in plane deformation and C–O stretching in the spectral region of 1440–1395 cm<sup>-1</sup> and 1315–1280 cm<sup>-1</sup>, respectively.<sup>36</sup> Compounds **1** and **2** show the  $\delta(\text{O}–\text{H})$  vibration at 1430 and 1431 cm<sup>-1</sup>, respectively, while in compound **3** the strong absorption at 1427 cm<sup>-1</sup> was assigned to a N–H deformation in plane correspondent to the C–O...H–N intermolecular hydrogen bonding (Figure 3). All compounds showed the C–O stretching at 1312 cm<sup>-1</sup>.

Strong bands observed for **1**, **2** and **3** near 750 cm<sup>-1</sup> were attributed to the C–H out-of-plane deformation and the very strong absorptions observed at 1597–1611 cm<sup>-1</sup> were assigned to the C=C axial deformation, both characteristic of aromatic compounds.<sup>38</sup>

#### UV-Vis spectra

The UV-Vis spectra of **1**, **2** and **3** dissolved in methanol were analyzed in the 190–440 nm spectral region. The assignments made for the main absorptions are based on literature data.<sup>39,40</sup> Aryl and/or phenyl-substituted triazenes show maximum absorptions at 190–440 nm

demonstrating their efficient chromophoric behavior. The electronic spectra of **1**, **2** and **3** were compared with those recorded in methanol for the compounds 1,3-bis(4-carboxyphenyl)triazene (**4**), 1,3-bis(4-fluorophenyl)triazene (**5**) and 1,3-bis(4-acetamidophenyl)triazene (**6**) respectively (Figure 1). The electronic spectra of compounds **4**, **5** and **6** dissolved in solvents with different polarities showed solvatochromism related to the n→ $\pi^*$  absorption due to the electron-withdrawing or donating property of fragments attached to terminal aryl substituents of the [–N=N–N(H)–] diazoamino group. Dissolved in methanol, **4**, **5** and **6** showed a  $\lambda_{\text{max}}$  value of 348, 351 and 369 nm assigned to this n→ $\pi^*$  absorption, respectively.<sup>38</sup> These values agree with the maximum observed of 361 nm for **1**, **2** and **3**. Further, the band observed at 242, 237 and 233 nm in the spectra of **1**, **2** and **3** respectively is attributed to the  $\pi \rightarrow \pi^*$  transition for aromatic rings, which were observed for **4** and **5** at 221 and 231 nm, respectively.<sup>38</sup> A third intense band observed near 200 nm for **1**, **2** and **3** was attributed to the n→ $\sigma^*$  transition of the carbonyl group.<sup>40</sup>

#### X-ray crystallography

Since the molecular association promoted by hydrogen bonding plays an important role in biological systems, especially for molecular recognition and reactivity of molecules with biological importance, the crystal structure analysis of one of the triazene derivatives was carried out to help understand the hydrogen bond network established by the terminal aryl group substituents of the [–N=N–N(H)–] diazoamino moiety, as well as the influence of this non-covalent interaction on the planarity of the molecule in the solid state. Attempts to obtain single crystals suitable for structural analysis of **1** and **2** are in progress.

Crystal data and experimental parameters of the structural analysis of **3** are presented in Table 1. Selected bond distances and angles are listed in Table 2. Figure 2 shows a projection of the molecular structure of FC<sub>6</sub>H<sub>4</sub>N=N(H)C<sub>6</sub>H<sub>4</sub>C(=O)NH<sub>2</sub> (**3**), while Figure 3 represents a section of the one-dimensional assembly of the molecules via secondary N–H...O, N–H...F, N–H...N and C–H...O hydrogen bonds, in a projection slightly tilted toward the [001] crystallographic direction.

Compound **3** crystallizes in the monoclinic crystal system, the non-centrosymmetric polar space group *Cc*. To test if a higher symmetry was eventually missed, an attempt was made to solve the structure in the centrosymmetric *C2/c* group, with negative results. Since the molecule of **3** is built only by light atoms that do not cause anomalous scattering, no significant intensity difference between the Friedel pairs *hkl* and *-h-k-l* could be observed in the collected reflection data. In other words, no conclusions could be drawn

**Table 1.** Crystal and structure refinement data for **3**

Empirical formula	C <sub>13</sub> H <sub>11</sub> FN <sub>4</sub> O
Formula weight	258.26
T (K)	150(2)
Radiation, λ (Å)	0.71073
Crystal system, space group	monoclinic, <i>Cc</i>
Unit cell dimensions, <i>a</i> , <i>b</i> , <i>c</i> (Å)	<i>a</i> = 27.630(2) <i>b</i> = 5.0682(4) <i>c</i> = 18.7030(17)
	β = 112.570(8)°
Volume (Å <sup>3</sup> )	2418.5(3)
Z	8
Calculated density (g cm <sup>-3</sup> )	1.419
Absorption coefficient (mm <sup>-1</sup> )	0.105
F(000)	1072
Crystal size (mm)	0.43 × 0.39 × 0.22
Theta range (°)	1.60 to 30.19
Index ranges	-38 ≤ <i>h</i> ≤ 38, -7 ≤ <i>k</i> ≤ 7, -26 ≤ <i>l</i> ≤ 26
Reflections collected	24746
Independent reflections	7113 [R <sub>int</sub> = 0.0362]
Completeness to theta	99.5 %
Max. and min. transmission	0.9772 and 0.9561
Refinement method	Full-matrix least-squares on F <sup>2</sup>
Data / restraints / parameters	7113 / 2 / 431
Goodness-of-fit on F <sup>2</sup>	1.067
Final R indices [I > 2σ (I)]	R <sub>1</sub> = 0.0433, wR <sub>2</sub> = 0.0994
R indices (all data)	R <sub>1</sub> = 0.0595, wR <sub>2</sub> = 0.1084
Largest diff. peak and hole (e.Å <sup>-3</sup> )	0.231 <sup>+</sup> and 0.195 <sup>-</sup>

\*Highest peak: 0.231 (e.Å<sup>-3</sup>) at 0.1935, 0.6264, 0.0511 [0.77 Å from H4].  
\*Deepest hole: -0.195 (e.Å<sup>-3</sup>) at 0.0306, 0.3744, 0.3387 [0.68 Å from N12].

about the orientation of the molecules relative to the polar axes in the unit cell of **3**. Two symmetrically independent molecules of **3** were observed in the asymmetric unit of the unit cell (Figure 2). The observed intermolecular hydrogen bonding involving the amide group made the independent molecules deviate from planarity, becoming chiral. The lack of planarity can be observed by the interplanar angles O1C1N1/C21–C26 [22.5(3)°; whole molecule r.m.s. deviation = 0.1610 Å] and O2C2N2/C41–C46 [2.7(3)°; whole molecule r.m.s. deviation = 0.0310 Å].

The molecular structure corresponds to the expected *trans* stereochemistry about the N11=N12 and N21=N22 double bonds. Diaryltriazenes typically present a delocalization of the π electrons of the triazene group towards the terminal aryl substituents. This property is supported by the deviations observed from normal N–N

**Table 2.** Selected bond lengths [Å] and angles [°] for **3**

Bond lengths	[Å]	Bond lengths	[Å]
C1–O1	1.248(2)	C2–O2	1.234(2)
C1–N1	1.327(2)	C2–N2	1.336(3)
C1–C24	1.485(2)	C2–C44	1.490(2)
C12–F1	1.361(2)	C32–F2	1.349(2)
N1–H3	0.81(3)	N2–H5	0.83(3)
N1–H4	1.02(3)	N2–H6	1.06(3)
N13–H1	1.01(3)	N23–H2	0.88(3)
N11–N12	1.280(2)	N21–N22	1.271(2)
N12–N13	1.327(2)	N22–N23	1.335(2)
Bond angles	[°]	Bond angles	[°]
O1–C1–N1	121.29(17)	O2–C2–N2	121.04(17)
O1–C1–C24	120.06(15)	O2–C2–C44	119.87(17)
N1–C1–C24	118.60(14)	N2–C2–C44	119.08(16)
F1–C12–C13	118.12(18)	F2–C32–C33	118.48(16)
F1–C12–C11	118.44(17)	F2–C32–C31	118.54(15)
C25–C24–C1	119.31(14)	C45–C44–C2	118.40(16)
C23–C24–C1	121.82(15)	C43–C44–C2	123.14(16)
C1–N1–H3	117.8(17)	C2–N2–H5	120.0(19)
C1–N1–H4	113.2(14)	C2–N2–H6	121.9(16)
H3–N1–H4	129(2)	H5–N2–H6	118(2)
N11–N12–N13	112.22(14)	N21–N22–N23	111.02(14)
N12–N13–H1	118(2)	N22–N23–H2	120.9(19)
C21–N13–H1	122(2)	C41–N23–H2	118.2(19)

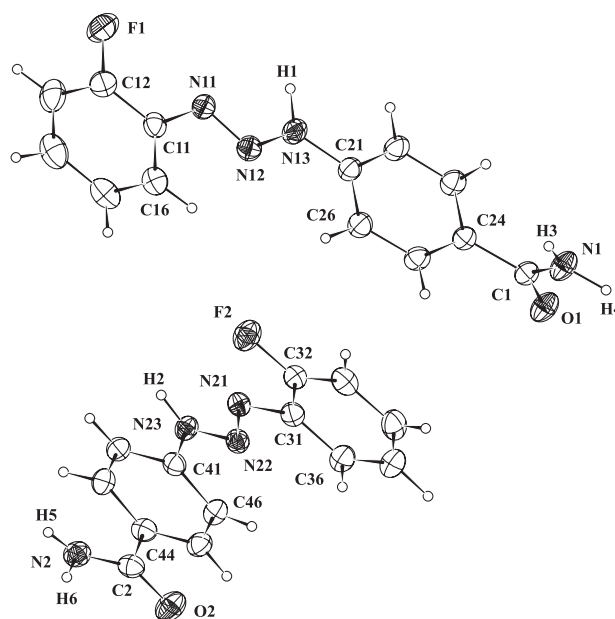


**Figure 2.** Molecular structure with atom-labeling scheme of the two symmetrically independent FC<sub>6</sub>H<sub>4</sub>N=N(H)C<sub>6</sub>H<sub>4</sub>C(=O)NH<sub>2</sub> molecules of **3** in the asymmetric unit of the space group *Cc*. Displacement ellipsoids are drawn at the 50% level.

and  $C_{\text{aryl}}-\text{N}$  bond lengths. Accordingly, the  $\text{N11}=\text{N12}$  [1.280(2) Å] and  $\text{N21}=\text{N22}$  [1.271(2) Å] bond lengths are longer than the characteristic value for a double bond (1.236 Å), whereas  $\text{N12}-\text{N13}$  [1.327(2) Å] and  $\text{N22}-\text{N23}$  [1.335(2) Å] bond distances are shorter than the characteristic value for a single bond (1.404 Å).<sup>41</sup> On the other hand,  $\text{C11}-\text{N11}$  [1.414(2) Å] and  $\text{C21}-\text{N13}$  [1.393(2) Å], as well as  $\text{C31}-\text{N21}$  [1.416(2) Å] and  $\text{C41}-\text{N23}$  [1.398(2) Å] bonds are shorter than the characteristic  $\text{N}-C_{\text{aryl}}$  single bonds (secondary amines,  $\text{R}_2\text{NH}$ ,  $\text{R}=\text{C}_{\text{sp}^2}$ ; 1.452 Å).<sup>42</sup> These values agree with those observed in similar compounds: 1,3-*bis*(2-trifluoromethylphenyl)triazene [ $\text{N}=\text{N}$  1.281(2) and  $\text{N}-\text{N}$  1.302(2) Å],<sup>40</sup> 1,3-*bis*(2,4-dibromophenyl)triazene [ $\text{N}=\text{N}$  1.267(7) and  $\text{N}-\text{N}$  1.332(7) Å],<sup>44</sup> and 1-(4-bromophenyl)-3-(4-nitrophenyl)triazene [ $\text{N}=\text{N}$  1.257(8) and  $\text{N}-\text{N}$  1.326(10) Å].<sup>43</sup> The bond angles of the  $\text{N}=\text{N}-\text{N}$  triad [ $\text{N11}-\text{N12}-\text{N13}$  112.22(14)°] and [ $\text{N21}-\text{N22}-\text{N23}$  111.02(14)°] are very close to the angles found in 1,3-*bis*(2-trifluoromethylphenyl)triazene [111.89(14)°] and 1-(4-bromophenyl)-3-(4-nitrophenyl)triazene [110.9(7)°].<sup>43,45</sup>

The PLATON software was used to analyze the intermolecular hydrogen bonding observed in the crystal of **3**, as shown in Figure 3.<sup>46</sup>

The crystal structure shows that the symmetrically independent  $\text{FC}_6\text{H}_4\text{N}=\text{N}(\text{H})\text{C}_6\text{H}_4\text{C}(=\text{O})\text{NH}_2$  molecules are individually related to each other by translation into

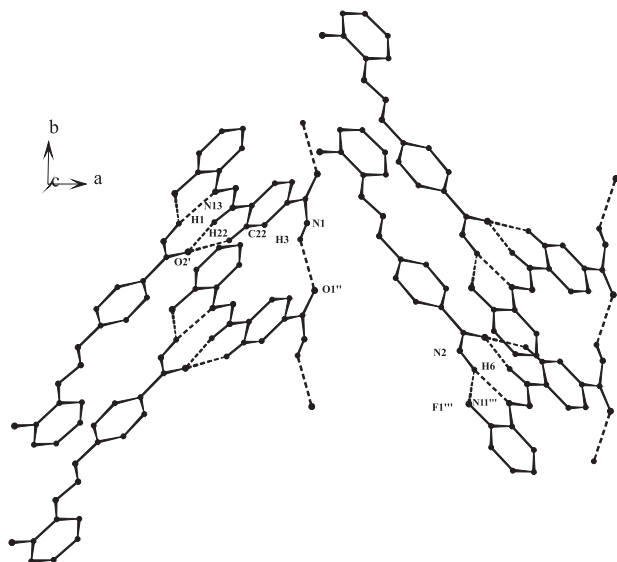


**Figure 3.** Section of the one-dimensional (1-D) assembling of the molecules in the crystal structure of  $\text{FC}_6\text{H}_4\text{N}=\text{N}(\text{H})\text{C}_6\text{H}_4\text{C}(=\text{O})\text{NH}_2$  (**3**). Intermolecular hydrogen bonds including bifurcated acceptor geometry ( $\text{D}_1-\text{H}_1, \text{D}_2-\text{H}_2$ ) $\cdots\text{A}$  ( $\text{D}$  = donor,  $\text{A}$  = acceptor atom), ( $\text{N13}-\text{H1}, \text{C22}-\text{H22}$ ) $\cdots\text{O2}'$ , bifurcated donor geometry  $\text{D}-\text{H}\cdots(\text{A}_1, \text{A}_2)$ ,  $\text{N2}-\text{H6}\cdots(\text{F1}''', \text{N11}''')$ , and classical  $\text{N1}-\text{H3}\cdots\text{O1}''$  hydrogen bonding along the crystallographic direction [010] are drawn with dashed lines. Symmetry transformations used to generate equivalent atoms: (')  $-1/2+x, -3/2-y, -1/2+z$ , (")  $x, -1+y, z$ , (""')  $1/2+x, -3/2-y, 1/2+z$ .

chains along the crystallographic direction [010]. Table 3 lists the geometric parameters of the intermolecular hydrogen-bonding in **3**. The molecules are associated through hydrogen bonds including a bifurcated acceptor geometry ( $\text{D}_1-\text{H}_1, \text{D}_2-\text{H}_2$ ) $\cdots\text{A}$  ( $\text{D}$  = donor,  $\text{A}$  = acceptor atom), ( $\text{N13}-\text{H1}, \text{C22}-\text{H22}$ ) $\cdots\text{O2}'$ , and a bifurcated donor geometry  $\text{D}-\text{H}\cdots(\text{A}_1, \text{A}_2)$ ,  $\text{N2}-\text{H6}\cdots(\text{F1}''', \text{N11}''')$ ; symmetry codes: (')  $-1/2+x, -3/2-y, -1/2+z$ , (""')  $1/2+x, -3/2-y, 1/2+z$ . The angle  $\text{F1}'''\cdots\text{H6}\cdots\text{N11}'''$  is 70.4(8)° and the elevation of  $\text{H6}$  from the plane defined by the atoms  $\text{F1}''', \text{N2}, \text{N11}'''$  is 0.02(3) Å. Atom  $\text{O2}'$  deviates 0.054(2) Å from the best plane defined by the atoms  $\text{C22}, \text{C2}', \text{N13}$ , while the angle  $\text{H1}\cdots\text{O2}'\cdots\text{H22}$  is 63(1)°. The one-dimensional arrangement of each symmetrically independent molecule of **3** along the crystallographic direction [010] results from the classical  $\text{N1}-\text{H3}\cdots\text{O1}''$  hydrogen bond, symmetry code: (")  $x, -1+y, z$ . Due to the symmetry independence of each molecule of **3**, which originates the 1-D arrangement, both chains running in opposite directions to each other along the crystallographic  $b$  axis are also symmetrically independent, as indicated in Figure 3.

**Table 3.** Hydrogen-bonding geometric parameters (Å, °) for **3**

$\text{D}-\text{H}\cdots\text{A}$	$\text{D}-\text{H}$	$\text{H}\cdots\text{A}$	$\text{D}\cdots\text{A}$	$\angle\text{D}-\text{H}\cdots\text{A}$
$\text{N13}-\text{H1}\cdots\text{O2}'$	1.01(3)	1.78(3)	2.758(2)	162(3)
$\text{C22}-\text{H22}\cdots\text{O2}'$	0.97(3)	2.52(2)	3.295(2)	136(2)
$\text{N2}-\text{H6}\cdots\text{F1}'''$	1.06(3)	2.51(3)	3.223(2)	123(2)
$\text{N2}-\text{H6}\cdots\text{N11}'''$	1.06(3)	2.10(3)	3.142(2)	166(2)
$\text{N1}-\text{H3}\cdots\text{O1}''$	0.81(3)	2.31(3)	2.963(2)	139(2)

( $\text{D}$  = donor atom,  $\text{A}$  = acceptor atom). Symmetry codes: (')  $-1/2+x, -3/2-y, -1/2+z$ , (")  $x, -1+y, z$ , (""')  $1/2+x, -3/2-y, 1/2+z$ .

### Biological activity

The ability of triazenes **1** and **2** to cleave supercoiled pUC 18 and pBSKII plasmids in pH 8.0 (200 mmol  $\text{L}^{-1}$  Tris-HCl buffer) upon incubation at 50 °C for 24 h is evidenced in Figure 4, while Figure S1 (see Supplementary Information) shows that triazene **3** promotes DNA cleavage in pH 6.5 (200 mmol  $\text{L}^{-1}$  PIPES buffer) after 24 h at 37 and 50 °C. Compounds **1** and **2** are able to cleave plasmid DNA by transforming the supercoiled form (**FI**) into the circular relaxed form **II** by single strand scission, while compound **3** was not able to show cleavage activity in the same conditions employed for **1** and **2**. However, compound **3** has demonstrated more cleavage efficiency in pH 6.5 after 24 h at 37 and 50 °C, due to additional cleavage of form **II** into **III** (linear form) as shown in Figure S1. The shape of the linear form can be attributed to an increase in the number of random cleavage events indicating low selectivity.<sup>47</sup>

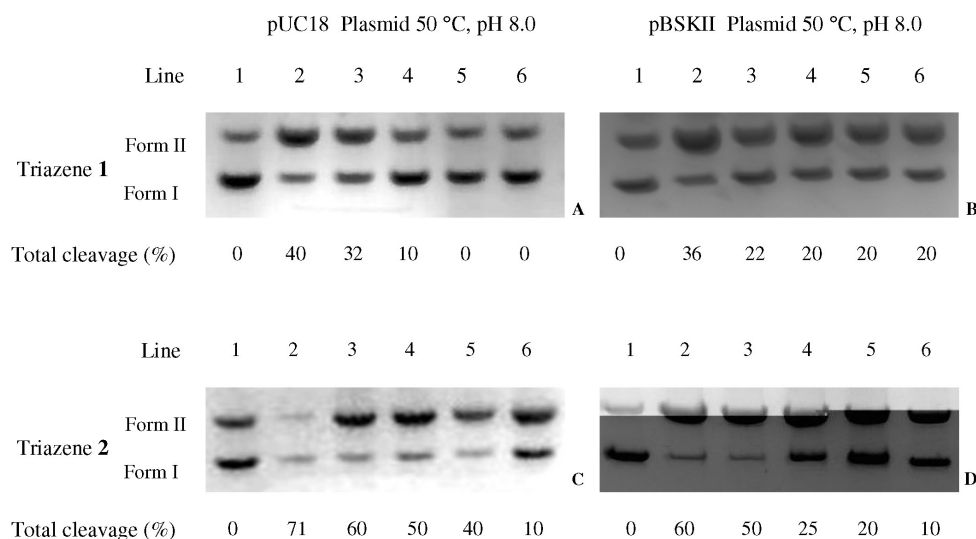


**Figure 4.** Total cleavage (%) of pUC18 and pBSKII plasmid DNA by triazenes **1** and **2**. Lane 1: control plasmid DNA (untreated pUC18 and pBSKII); lanes 2-6: addition of compounds in different concentrations: 3.75, 1.875, 1.25, 0.75 and 0.375 mmol L<sup>-1</sup>. Incubation for 24 h at 50 °C, pH 8.0.

In order to verify the plasmid DNA cleavage mechanism for **1**, **2** and **3**, assays were carried out in the presence of 0.04 mol L<sup>-1</sup> dmsol or 0.1-1.0% glycerol as hydroxyl radical scavengers. The experiments showed that these conditions did not affect the cleavage activity of **1**, **2** and **3**, suggesting that free hydroxyl radicals do not participate in the cleavage reaction.<sup>48,49</sup> To confirm that molecular oxygen did not participate in the reaction, other assays were conducted under anaerobic conditions, showing that the cleavage ability of **1**, **2** and **3** is not based on an oxidative mechanism. In conclusion, the plasmid DNA cleavage activity of **1**, **2** and **3** is probably based on a hydrolytic mechanism. It is important to point out that all natural nucleases act through a hydrolytic mechanism.<sup>47</sup>

The MIC values of **1**, **2** and **3** showed weak activity against Gram-positive and Gram-negative bacteria. Two susceptibility endpoints were recorded for each isolate. The MIC is the lowest concentration of the compound in which the microorganism does not demonstrate visible growth. Minimum bactericidal concentration (MBC), in its turn, is defined as the lowest concentration yielding negative subculture or only one colony. The results show that **1** is the most active triazene, inhibiting the growth of some strains with MIC values of 128 µg mL<sup>-1</sup> (*Enterococcus faecalis* ATCC 29212, *Klebsiella oxytoca* and *Aeromonas hydrophyla*) and 32 µg mL<sup>-1</sup> for *Bacillus cereus*. Compound **2** revealed a MIC value of 64 µg mL<sup>-1</sup> for *Streptococcus agalactiae*, while triazene **3** did not show promising antimicrobial activity (MIC values higher than 128 µg mL<sup>-1</sup> against all bacteria assessed). The MBC values for **1**, **2** and **3** were higher than 128 µg mL<sup>-1</sup> for all organisms investigated. The observed MICs of **1**, **2** and **3**

against the tested organisms are comparable to those of the similar compounds 1-(2-fluorophenyl)-3-(4-acetylphenyl) triazene, 1-(4-ethoxyphenyl)-3-(4-carboxyphenyl) triazene, 1-(4-nitrophenyl)-3-(4-carboxyphenyl) triazene and 1-(4-acetylamino phenyl)-3-(4-carboxyphenyl) triazene.<sup>25</sup> Other studies have shown that triazenes have better activity against gram-positive than gram-negative bacteria,<sup>24</sup> given the fact that the gram-negative bacterial membrane is more complex than the gram-positive one and presents a barrier to the penetration of numerous antimicrobial molecules. Also, the periplasmic space contains large concentrations of enzymes which are able to decompose exogenous molecules. However, the mode of action of the reported compounds is still undetailed.

Most anticancer agents act on DNA or its precursors, inhibiting their synthesis or causing irreparable damage to their molecules. Examples are alkylating agents, cisplatin and antibiotics with antitumor activity, which are able to act at various cell cycle phases and are called non phase-specific. In this context, the bleomycins A<sub>2</sub> and B<sub>2</sub> form an important group of antibiotics able to cleave DNA through an oxidative mechanism.<sup>50</sup> The cytotoxic action of bleomycin transformed it into an anticancer drug with significant activity against squamous cell carcinoma of the uterine cervix, lymphomas and testicular tumors. Other examples of antibiotics used in anticancer therapy are dactinomycin, daunorubicin, doxorubicin, epirubicin, mitoxantrone, idarubicin and doxorubicin (or adriamycin).<sup>50,51</sup> The default schema for the Hodgkin's disease treatment consists of the combination chemotherapy of adriamycin, bleomycin, vinblastine and dacarbazine (ABVD).<sup>52</sup>

The ability of the triazenes **1**, **2** and **3** to kill human cancer cells was investigated using marrow bone cultures of leukemia patients and peripheral blood of control patient with a standard bioassay, MTT. Cells were exposed to **1**, **2** and **3** during 24 h in order to evaluate the effects of the investigated triazenes as described in the experimental section. For comparison purposes, DTIC cytotoxicity was evaluated under the same conditions. Based on the concentration-response curve, the cell survival did not depend on the triazene concentration for compounds **1**, **2** and **3** (Figure 5).

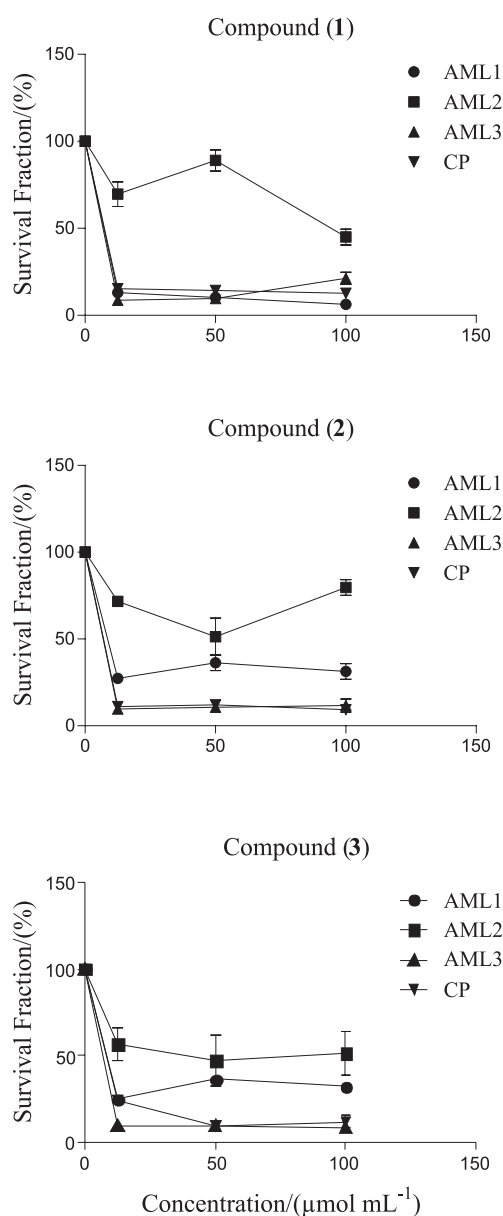


**Figure 5.** Concentration dependence of the effect of the **1**, **2** and **3** triazenes on cell proliferation of acute myeloid leukemia (AML1, AML2, AML3) and normal leukocytes (CP). Cells were exposed and viability determined after 24 h. Each data point represents the arithmetic mean  $\pm$  standard deviation.

Table 4 shows the results of the antiproliferative effect of **1**, **2** and **3** on acute myeloid leukemia cells and control patient cells. IC<sub>50</sub> values in the range of 1.83-129.30 μmol mL<sup>-1</sup> were observed for the leukemia cells. The compounds **1**, **2** and **3** demonstrated cytotoxicity very similar against AML3, while compound **1** appeared to be more cytotoxic than **2** and **3** against AML1. These results suggest that the replacement of fluorine by chlorine in compound **1** increased the antileukemic activity of the triazenes in all leukemic cells tested. Against AML3 cells the compounds presented the best anti-leukemic activity and against AML2 the worst. However, the three compounds were more active against AML2 cells compared to DTIC. The correct dose is one of the most important aspects to achieve the best antitumor effect without increasing toxicity too much, considering that the therapeutic window of most antineoplastic agents is narrow. The fact that the IC<sub>50</sub> of the three compounds for AML3 is half the CP allows us to suggest the possibility of administering a lower dosage, reducing toxicity. Data also showed that the compounds evaluated were highly toxic to normal leukocytes. The results of the MTT-dye reduction assay indicated that **1**, **2** and **3** had a significant cytotoxic/antiproliferative effect in comparison with other triazenes.<sup>53,54</sup>

The three triazene compounds described in this work belong to the alkylating agents group with similar chemical, physical, antimicrobial, nuclease and antitumor properties. DTIC and TMZ also belong to this group, showing an activity mechanism mainly related to the methylation of

**Table 4.** Inhibition of cell growth by triazenes **1**, **2** and **3** and DTIC assessed after 24 h exposure (MTT-dye reduction assay)

Compound	Tumor cell	IC <sub>50</sub> (μmol mL <sup>-1</sup> ) <sup>(a)</sup>
<b>1</b>	AML1 <sup>(b)</sup>	2.33
	AML2 <sup>(c)</sup>	116.6
	AML3 <sup>(d)</sup>	1.99
	CP <sup>(e)</sup>	3.17
<b>2</b>	AML1 <sup>(b)</sup>	10.73
	AML2 <sup>(c)</sup>	129.3
	AML3 <sup>(d)</sup>	1.95
	CP <sup>(e)</sup>	2.17
<b>3</b>	AML1 <sup>(b)</sup>	9.67
	AML2 <sup>(c)</sup>	47.86
	AML3 <sup>(d)</sup>	1.83
	CP <sup>(e)</sup>	4.44
<b>DTIC</b>	AML2 <sup>(c)</sup>	132.4

<sup>(a)</sup>IC<sub>50</sub> (dose required to achieve 50% decrease in cell growth). <sup>(b)</sup>AML1 = acute myeloid leukemia cells of patient number 1. <sup>(c)</sup>AML2 = acute myeloid leukemia cells of patient 2. <sup>(d)</sup>AML3 = acute myeloid leukemia cells of patient 3. <sup>(e)</sup>CP = control patient cells of peripheral blood.

*O*<sup>6</sup>-guanine, mediated by the methyldiazonium ion, a highly reactive derivative of these chemotherapeutic agents. The antitumor effects of alkylating agents and cell resistance to them depend on at least three DNA repair systems: a) increase in *O*<sup>6</sup>-methyl-guanine methyl-transferase (MGMT), also called *O*<sup>6</sup>-alkylguanine-DNA-alkyltransferase; b) loss of mismatch repair (the MMR system recognizes and repairs base-base mismatches and small insertion-deletions loops, IDLs); and c) base excision repair (BER) deficiency.

## Conclusions

The 1-(2-chlorophenyl)-3-(4-carboxyphenyl)triazene (**1**), 1-(2-fluorophenyl)-3-(4-carboxyphenyl)triazene (**2**) and 1-(2-fluorophenyl)-3-(4-amidophenyl)triazene (**3**) compounds assessed in the present study are capable to cleave plasmid DNA under defined pH, temperature and time conditions. Since the efficiency of plasmid DNA cleavage by the investigated triazenes was not inhibited in the presence of free hydroxyl scavengers and anaerobic atmosphere conditions, the hydrolytic mechanism for the DNA reaction is suggested, a mechanism similar to the one promoted by natural nucleases. The experimental results indicated that triazenes **1** and **2** had considerable action against gram-positive bacteria. All compounds tested had pronounced cytotoxic activity against acute myeloid leukemia cells and normal leukocytes. Further studies to establish whether methylated triazene compounds in human leukemia could offer a new approach to control this disease are required. The crystal and molecular structure of one of the triazene derivatives (**3**) revealed intramolecular and intermolecular interactions promoted by hydrogen bonding, which establish a significant influence on the molecular planarity in the solid state. This observation suggests that **3** is probably not susceptible to DNA binding by intercalation. The presence of fluorine and amide substituents favor hydrogen bonding, indicating that the mode of action of **3** may involve an hydrolytic mechanism initiated by an external approach directed to the major or minor grooves of the DNA molecule.

## Supplementary Information

Crystallographic data for the structural analysis have been deposited with the Cambridge Crystallographic Data Centre (CCDC no. 751661). Further details of the crystal structure investigation are available free of charge via [www.ccdc.cam.ac.uk/conts/retrieving.html](http://www.ccdc.cam.ac.uk/conts/retrieving.html) (or from the CCDC, 12 Union Road, Cambridge CB2 1EZ, UK; fax: +44 1223 336033; e-mail: [deposit@ccdc.cam.ac.uk](mailto:deposit@ccdc.cam.ac.uk)).

Table S1 and Figure S1 are available free of charge at <http://jbcs.s bq.org.br>, as pdf file.

## Acknowledgements

M. H. thanks CNPq (proc. 305254/2009-0), F. K. thanks CNPq/PIBIC, A. L. thanks CNPq and V. F. G. thanks CAPES for grants. The diffractometer was supported by the Financiadora de Estudos e Projetos (FINEP, CT-INFRA 03/2001). The authors are grateful to PRPGP/UFSP/Pró-Publicações Internacionais for the language review of the manuscript.

## References

1. Khranov, D. M.; Belawski, C. W.; *J. Org. Chem.* **2007**, *72*, 9407.
2. Rouzer, C. A.; Sabourin, M.; Skinner, T. L.; Thompson, E. J.; Wood, T. O.; Chmurny, G. N.; Klose, J. R.; Roman, J. M.; Smith, R. H. Jr.; Michejda, C. J.; *Chem. Res. Toxicol.* **1996**, *9*, 172.
3. Nicolaou, K. C.; Boddy, C. N. C.; Li, H.; Koumbis, A. E.; Hughes, R.; Natarajan, S.; Jain, N. F.; Ramanjulu, J. M.; Bräse, S.; Solomon, E.; *Chem. Eur. J.* **1999**, *5*, 2602.
4. Bräse, S.; Dahmen, S.; Pfefferkorn, M.; *J. Comb. Chem.* **2000**, *2*, 710.
5. Jones II, L.; Schumm, J. S.; Tour, J. M.; *J. Org. Chem.* **1997**, *62*, 1388.
6. Moore, J. S.; *Acc. Chem. Res.* **1997**, *30*, 402.
7. Jean-Claude, B. J.; Mustafa, A.; Damian, Z.; De Marte, J.; Vasillescu, D. E.; Yen, R.; Chan, T. H.; Leyland-Jones, B.; *Biochem. Pharmacol.* **1999**, *57*, 753.
8. Doucet, K. G.; Pye, C. C.; Vaughan, K.; Enright, T. G.; *THEOCHEM* **2006**, *801*, 21.
9. An, Y.; Liu, S.; Deng, S.; Ji, L.; Mao, Z.; *J. Inorg. Biochem.* **2006**, *100*, 1586.
10. Shao, Y.; Ding, Y.; Jia, Z.; Lu, X.; Ke, Z.; Xu, W.; Lu, G.; *Bioorg. Med. Chem.* **2009**, *17*, 4274.
11. Takasaki, B. K.; Jik Chin, J.; *J. Am. Chem. Soc.* **1994**, *116*, 1122.
12. Burr, S. J.; Mselati, A.; Thomas, E. W.; *Tetrahedron Lett.* **2003**, *44*, 7307.
13. O' Reilly, S. M.; Newlands, E. S.; Glaser, M. G.; Brampton, M.; Rice-Edwards, J. M.; Illingworth, R. D.; Richards, P. G.; Kennard, C.; Colquhoun, I. R.; Lewis, P.; Stevens, M. F. G.; *Eur. J. Cancer* **1993**, *29A*, 940.
14. Bleehen, N. M.; Newlands, E. S.; Lee, S. M.; Thatcher, N.; Selby, P.; Calvert, A. H.; Rustin, G. J.; Brampton, M.; Stevens, M. F.; *J. Clin. Oncol.* **1995**, *13*, 910.
15. Hoang-Xuan, K.; Camilleri-Broet, S.; Soussain, C.; *Curr. Opin. Oncol.* **2004**, *16*, 601.
16. Tani, M.; Fina, M.; Alinari, L.; Stefoni, V.; Baccarani, M.; Zinzani, P. L.; *Haematologica* **2005**, *90*, 1283.
17. Kanjeekal, S.; Chambers, A.; Fung, M. F.; Verma, S.; *Gynecol. Oncol.* **2005**, *97*, 624.

18. D'Incalci, M.; Souteyrand, P.; *Ann. Dermatol. Venereol.* **2001**, *128*, 517.
19. Perry, M. J.; Mendes, E.; Simplício, A. L.; Coelho, A.; Soares, R. V.; Iley, J.; Moreira, R.; Francisco, A. P.; *Eur. J. Med. Chem.* **2009**, *44*, 3228.
20. Rijn, J. V.; Heimans, J. J.; Berg, J. V. D.; Valk, P. V. D.; Slotman, B. J.; *J. Rad. Oncol. Biol. Phys.* **2000**, *47*, 779.
21. Franchi, A.; Papa, G.; D'ATri, S.; Piccioni, D.; Masi, M.; Bonmassar, E.; *Haematologica* **1992**, *77*, 146.
22. Seiter, K.; Liu, D.; Loughran, T.; Siddiqui, A.; Baskind, P.; Ahmed, T.; *J. Oncol.* **2002**, *20*, 3249.
23. Seiter, K.; Liu, D.; Siddiqui, A. D.; Lerner, R.; Nelson, J.; Ahmed, T.; *Leuk. Lymph.* **2004**, *45*, 1209.
24. Hörner, M.; Giglio, V. F.; Santos, A. J. R. W.; Westphalen, A. B.; Iglesias, B. A.; Martins, P. R.; Amaral, C. H.; Michelot, T. M.; Reetz, L. G. B.; Bertoncheli, C. M.; Paraginski, G. L.; Hörner, R.; *Braz. J. Pharm. Sci.* **2008**, *44*, 441.
25. Marchesi, F.; Turriziani, M.; Tortorelli, G.; Avvisati, G.; Torino, F.; De Vecchis, L.; *Pharm. Res.* **2007**, *56*, 275.
26. Desiraju, G. R.; Steiner, T.; *The Weak Hydrogen Bond in Structural Chemistry and Biology*, IUCr Monographs on Crystallography 9, Oxford University Press Inc: New York, 1999.
27. Steiner, T.; *Angew. Chem., Int. Ed.* **2002**, *41*, 48.
28. Grammaticakis, P.; *Bull. Soc. Chim. Fr.* **1956**, 139.
29. Horn Jr., A.; Vencato, I.; Bortoluzzi, A. J.; Hörner, R.; Silva, R. A. N.; Spoganicz, B.; Drago, V.; Terenzi, H.; Oliveira, M. C. B.; Werner, R.; Haase, W.; Neves, A.; *Inorg. Chim. Acta* **2005**, *358*, 339.
30. Clinical and Laboratory Standards Institute; *Methods for Dilution Antimicrobial Susceptibility Tests for Bacteria that Grow Aerobically*. Approved Standard; 6<sup>th</sup> ed.; Wayne: NCCLS, 2003; p.53. (NCCLS document M7-A6).
31. Beloti, V.; Barros, M. A. F.; Freitas, J. C.; Nero, L. A.; Souza, J. A.; Santana, E. H. W.; Franco, B. D. G. M.; *Rev. Microbiol.* **1999**, *30*, 137.
32. COSMO (Version 1.48), SAINT (Version 7.06°), SADABS (Version 2.10); Bruker AXS Inc.; Madison: Wisconsin, USA, 2005.
33. Burla, M. C.; Caliandro, R.; Camalli, M.; Carrozzini, B.; Cascarano, G. L.; De Caro, L.; Giacovazzo, C.; Polidori, G.; Spagna, R.; (SIR2004) *J. Appl. Crystallogr.* **2005**, *38*, 381.
34. Sheldrick, G. M.; *SHELXL-97; Program for Crystal Structure Refinement*; University of Göttingen, Germany, 1997.
35. Brandenburg, K.; *DIAMOND 3.1a*. 1997-2005; Crystal Impact GbR, Bonn, Germany, 1997.
36. Colthup, N. B.; Daly, L. H.; Wiberley, S. E.; *Introduction to Infrared and Raman Spectroscopy*, 3<sup>rd</sup> ed., Academic Press: New York, 1990.
37. Kübler, R.; Lüttke, W.; Weckherlin, S.; *Z. Elektrochem.* **1960**, *64*, 650.
38. Silverstein, R. M.; Webster, F. X.; *Spectrometric Identification of Organic Compounds*, 6<sup>th</sup> ed., John Wiley & Sons: New York, 1998.
39. Masoud, M. S.; Ali, A. E.; Shaker, M. A.; Ghani, M. A.; *Spectrochim. Acta* **2005**, *61A*, 3102.
40. Silverstein, R. M.; Bassler, G. C.; Morrill, T. C.; *Spectrometric Identification of Organic Compounds*, John Wiley & Sons: New York, 1981.
41. Allen, F. H.; Kennard, O.; Watson, D. G.; Brammer, L.; Orpen, A. G.; Taylor, R.; *J. Chem. Soc., Perkin Trans. I* **1987**, *2*, S1; Teatum, E.; Gschneider, K.; Waber, J.; Report LA-2345. Los Alamos Scientific Laboratory, New Mexico, USA, 1960.
42. Orpen, A. G.; Brammer, L.; Allen, F. H.; Kennard, O.; Watson, D. G.; Taylor, R.; *J. Chem. Soc., Dalton Trans.* **1989**, S1–83.
43. Hörner, M.; Silva, A.; Fenner, H.; *Anal. Sci.: X-ray Struct. Anal. Online* **2006**, *22*, x295.
44. Hörner, M.; Casagrande, I. C.; Bordinhão, J.; Mössmer, C. M.; *Acta Crystallogr.* **2002**, *C58*, o193.
45. Hörner, M.; Visentin, L. C.; Behm, M. B.; Machado, F. C.; Bortoluzzi, A. J.; *Anal. Sci.: X-ray Struct. Anal. Online* **2007**, *23*, x247.
46. Spek, A. L.; *PLATON, A Multipurpose Crystallographic Tool*, Utrecht University, Utrecht: The Netherlands, 2008.
47. Fernandes, C.; Parrilha, G. L.; Lessa, J. A.; Santiago, L. J. M.; Kanashiro, M. M.; Boniolo, F. S.; Bortoluzzi, A. J.; Vugman, N. V.; Herbst, M. H.; Horn Jr., A.; *Inorg. Chim. Acta* **2006**, *359*, 3176.
48. Basile, L. A.; Barton, J. K.; *J. Am. Chem. Soc.* **1987**, *109*, 7548.
49. Cowan, J. A.; *Curr. Opin. Chem. Biol.* **2001**, *5*, 634.
50. Brunton, L. L.; Lazo, J. S.; Parkker, K. L.; *Goodman & Gilman*, McGraw-Hill Interamericana do Brasil: Rio de Janeiro, 2006.
51. Gewirtz, D. A. A.; *Biochem. Pharmacol.* **1999**, *57*, 727.
52. Duggan, D. B.; Petroni, G. R.; Johnson, J. L.; Glick, J. H.; Fisher, R. I.; Connors, J. M.; Canellos, G. P.; Peterson B. A.; *J. Clin. Oncol.* **2003**, *21*, 607.
53. Smith, R. H.; Scudiero, D. A.; Michejda, C. J.; *J. Med. Chem.* **1990**, *33*, 2579.
54. Zheleva, A. M.; Gadjeva, V. G.; *Int. J. Pharm.* **2001**, *212*, 257.

Submitted: October 25, 2009

Published online: August 10, 2010

## In Vitro Evaluation of Triazenes: DNA Cleavage, Antibacterial Activity and Cytotoxicity against Acute Myeloid Leukemia Cells

**Vanessa O. Domingues,<sup>a</sup> Rosmari Hörner,<sup>\*a</sup> Luiz G. B. Reetz,<sup>a</sup> Fábio Kuhn,<sup>a</sup>  
 Virgínia M. Coser,<sup>b</sup> Jacqueline N. Rodrigues,<sup>b</sup> Rita Bauchspiess,<sup>b</sup>  
 Waldir V. Pereira,<sup>b</sup> Gustavo L. Paraginski,<sup>c</sup> Aline Locatelli,<sup>c</sup>  
 Juliana de O. Fank,<sup>c</sup> Vinícius F. Giglio<sup>c</sup> and Manfredo Hörner<sup>\*c</sup>**

<sup>a</sup> Universidade Federal de Santa Maria, Departamento de Análises Clínicas e Toxicológicas,  
 97105-970 Santa Maria-RS, Brazil

<sup>b</sup>Hospital Universitário de Santa Maria, Departamento de Hematologia-Oncologia,  
 97105-970 Santa Maria-RS, Brazil

<sup>c</sup> Universidade Federal de Santa Maria, Departamento de Química, C.P. 5031,  
 97105-970 Santa Maria-RS, Brazil

**Table S1.** Minimum inhibitory concentration values ( $\mu\text{g mL}^{-1}$ ) determined for the triazenes **1**, **2** and **3**

Bacterial strain	Compound 1	Compound 2	Compound 3
<i>Pseudomonas aeruginosa</i> ATCC 27853	> 128	> 128	> 128
<i>Escherichia coli</i> ATCC 25922	> 128	> 128	> 128
<i>Escherichia coli</i> ATCC 35218	> 128	> 128	> 128
<i>Salmonella choleraesuis</i> ATCC 10708	> 128	> 128	> 128
<i>Klebsiella pneumoniae</i> ATCC 700603	> 128	> 128	> 128
<i>Staphylococcus aureus</i> ATCC 25923	> 128	> 128	> 128
<i>Staphylococcus epidermidis</i> ATCC 12228	> 128	> 128	> 128
<i>Enterococcus faecalis</i> ATCC 29212	= 128	> 128	> 128
<i>Bacillus cereus</i> ATCC 10987	> 128	> 128	> 128
<i>Shigella sonnei</i>	> 128	> 128	> 128
<i>Enterobacter cloacae</i>	> 128	> 128	> 128
<i>Klebsiella oxytoca</i>	= 128	> 128	> 128
<i>Bacillus cereus</i>	= 32	> 128	> 128
<i>Micrococcus sp.</i>	> 128	> 128	> 128
<i>Streptococcus pyogenes</i>	> 128	> 128	> 128
<i>Acinetobacter baumannii</i>	> 128	> 128	> 128
<i>Raustonia pickettii</i>	> 128	> 128	> 128
<i>Serratia marcescens</i>	> 128	> 128	> 128
<i>Enterococcus sp.</i>	> 128	> 128	> 128
<i>Listeria monocytogenes</i>	> 128	> 128	> 128
<i>Aeromonas hydrophyla</i>	= 128	> 128	> 128
<i>Enterobacter aerogenes</i>	> 128	> 128	> 128
<i>Streptococcus agalactiae</i>	> 128	= 64	> 128
<i>Salmonella tiphymurium</i>	> 128	> 128	> 128
<i>Corynebacterium sp.</i>	> 128	>128	> 128
<i>Salmonella sp.</i>	> 128	>128	> 128
<i>Staphylococcus epidermidis</i>	> 128	> 128	> 128
<i>Acinetobacter lwoffii</i>	> 128	> 128	> 128
<i>Klebsiella pneumoniae</i>	> 128	> 128	> 128
<i>Staphylococcus hominis subsp. hominis</i>	> 128	> 128	> 128

\*e-mail: rosmari.ufsm@gmail.com, hoerner.manfredo@gmail.com

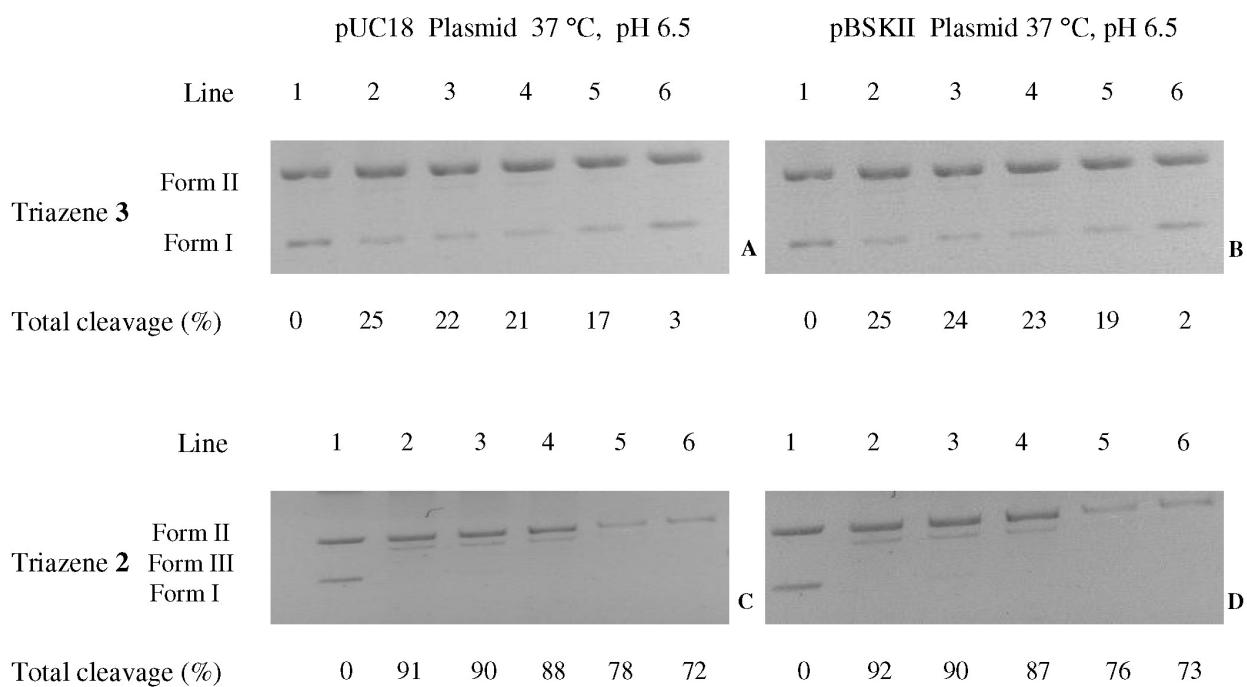


**Figure S1.** Total cleavage (%) of pUC18 and pBSKII plasmid DNA by triazene 3. Lane 1: control plasmid DNA (untreated pUC18 and pBSKII); Lanes 2-6: addition of compounds in different concentrations: 3.75, 1.875, 1.25, 0.75 and 0.375 mmol L<sup>-1</sup>. Incubation for 24 h at 37 and 50 °C, pH 6.5.